

## Analysis of stability of light beams in nonlinear photorefractive media

E. Infeld

*Soltan Institute for Nuclear Studies, Hoża 69, 00-681 Warsaw, Poland*

T. Lenkowska-Czerwińska

*IPPT, Polish Academy of Sciences, Świętokrzyska 21, 00-049 Warsaw, Poland*

(Received 18 November 1996)

We investigate the stability of both bright and dark beams propagating in bulk media with a photorefractive nonlinear response, such as crystals. The beams are seen to be unstable with respect to perturbations along the initially homogeneous coordinate. Our analysis is based on a  $k$  expansion for the perturbation. Agreement with recent numerical calculations is obtained. Growth rates obtained extend previous results into the small- $k$  region. In the case of bright beams the extension is straightforward, whereas for dark beams an interpretation is needed. We suggest an improvement of dark-beam laser-crystal devices, resulting in better stability of the beam. We comment on some recent experiments. [S1063-651X(97)06705-6]

PACS number(s): 42.65. Tg, 42.65. Jx, 42.65. Hw,

### I. INTRODUCTION

This paper treats instabilities of light beams propagating in nonlinear media. An example is the propagation of visible laser light along an axis of a photorefractive crystal. Self-trapping of light beams in such media is often studied theoretically and numerically by looking at solitary-wave solutions to relevant nonlinear model equations. The nonlinear Schrödinger equation was derived for optical beams in Kerr-type media some time ago. Exact (1+1)-dimensional solitary-wave solutions were seen to be unstable with respect to perpendicular perturbations [1,2]. For a comprehensive analysis, including nonlinear structures other than solitons and their stability, see [3,4]. The symmetry-breaking instability, also known as a transverse modulational instability, leads to a breakup of structure and has been investigated numerically and experimentally in many physical contexts [5–12].

Here we will perform a stability analysis of the perpendicular instability described above in bulk photorefractive media. Both bright stripe solitary solutions in focusing media and dark “solitons” in defocusing media are considered. It will transpire that, at least in the latter case, considering solitary-wave solutions alone is not sufficient.

The photorefractive nonlinearity is due to the static electric field generated by the optical beam. A derivation of the model equations that will be treated here can be found elsewhere [13]. They are for propagation of an optical beam with amplitude  $B(\mathbf{r})$  along a crystal axis in the presence of an external field, the magnitude of which has been absorbed in the variables:

$$\left[ \frac{\partial}{\partial x} - \frac{i}{2} \nabla_{\perp}^2 \right] B = is \frac{\partial \varphi}{\partial z} B, \quad (1)$$

$$\nabla_{\perp}^2 \varphi + \nabla_{\perp} \ln(1 + |B|^2) \nabla_{\perp} \varphi = \frac{\partial}{\partial z} \ln(1 + |B|^2). \quad (2)$$

Here  $\varphi$  is the normalized electrostatic potential induced by the beam and  $\nabla_{\perp} \varphi(r \rightarrow \infty) \rightarrow 0$ . The amplitude of the elec-

tromagnetic beam is  $B(\mathbf{r})$ . The operator  $\nabla_{\perp}$  acts on  $y$  and  $z$ . Normalizations are given in [13]. For a self-focusing medium  $s = +1$ , whereas  $s = -1$  for a self-defocusing medium such as a crystal of strontium barium niobate. The beam is propagating along  $x$  and initially its profile depends on  $z$  only. We will first look at possible shapes for the two families of beams and then at their stability with respect to long-wavelength perturbations along  $y$ . Our analysis will be linear in the perturbation. Thus further developments after breakup of the beam, such as the formation of vortices [11–16], will not be included in our theory so far.

### II. EXACT SOLUTIONS AS MODELS OF THE BEAMS

If both  $|B|$  and  $\varphi$  are functions of  $z$  only, Eq. (2) can be integrated to yield

$$\frac{\partial \varphi}{\partial z} = \frac{|B|^2 - B_0^2}{1 + |B|^2}, \quad (3)$$

where  $B_0^2$  is a constant. We can now obtain one equation for  $B(x, z)$ :

$$\left( \frac{\partial}{\partial x} - \frac{i}{2} \frac{\partial^2}{\partial z^2} \right) B = is \frac{|B|^2 - B_0^2}{1 + |B|^2} B. \quad (4)$$

We will start by looking for solutions for  $s = 1$ , corresponding to bright stripes. Take  $B(x, z) = e^{i\Gamma_0 x} b(z)$ ,  $B_0 = 0$ . Here  $\Gamma_0$  is the soliton propagation constant. It will prove convenient to write  $\Gamma_0 = 1 - b_m^{-2} \ln(1 + b_m^2)$ . We obtain (subscripts denote differentiation and  $b_{z=0}$  is the value of  $b_z$  at  $z = 0$ )

$$b_z^2 = b_{z=0}^2 + 2 \left[ \ln(1 + b^2) - \frac{b^2}{b_m^2} \ln(1 + b_m^2) \right], \quad (5)$$

$$2 - 2 \ln \alpha - \frac{2}{\alpha} \leq b_{z=0}^2 < \infty, \quad \alpha = \frac{b_m^2}{\ln(1 + b_m^2)}.$$

See [15] for the derivation. Soliton solutions correspond to  $b_{z=0}^2 = 0$ . They model a bright, symmetric beam with maxi-

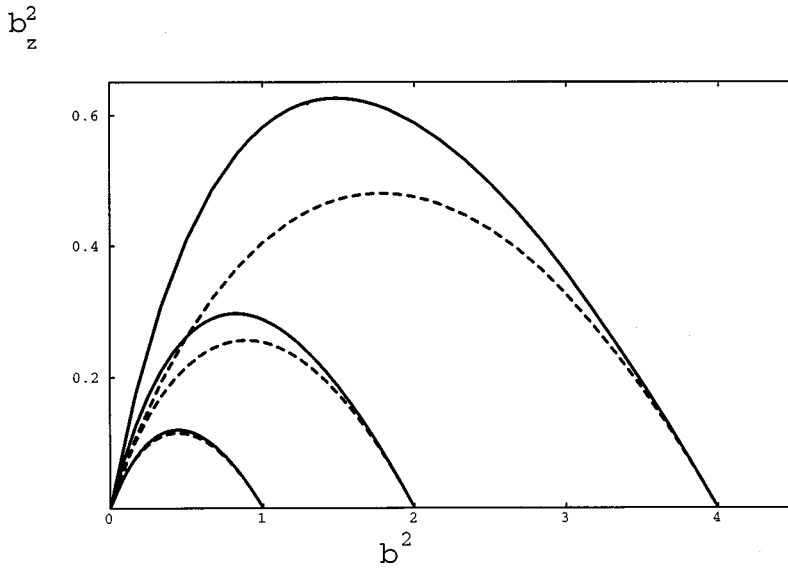


FIG. 1. Parametric  $b_z^2$  as a function of  $b^2$  for the bright soliton and  $b_m^2=1,2,4$  (continuous lines). Phase curves for the model function, defined in the text, are indicated as dashed lines. In this and following figures, all quantities are normalized as in [13] and so the variables are dimensionless.

mum intensity  $b_m$ . For  $b_{z0}^2$  negative, in which case it ceases to have a physical interpretation and just becomes a parameter in Eq. (5), we have  $b > 0$  for all  $z$  and the solution is periodic. For  $b_{z0}^2$  positive,  $b$  takes on both positive and negative values and  $b(z)$  is once again periodic. Various cases for the nonlinear Schrödinger equation, which is a limiting case of Eq. (4) for small  $|B|$ , are described and illustrated in Chap. 6 of Ref. [4]. The classification is similar here.

The dependence of  $b_z^2$  on  $b^2$  for the soliton case can be seen in Fig. 1 ( $b_{z0}^2=0$ , three values of  $b_m^2$ ). This parametric dependence is illustrated by continuous lines in the figure.

For the defocusing case  $s=-1$ , we take  $B_0=b_m$ ,  $\Gamma_0=0$ , and integrate Eq. (4) to obtain (see [15])

$$b_z^2 = b_{z0}^2 + 2[b^2 - (1 + b_m^2)\ln(1 + b^2)], \tag{6}$$

$$0 \leq b_{z0}^2 \leq 2[(1 + b_m^2)\ln(1 + b_m^2) - b_m^2]. \tag{7}$$

Here  $b_{z0}$  is always the  $z$  derivative of  $b$  at  $z=0$ . Taking  $\Gamma_0$  to be zero is not a serious restriction, as Eq. (6) can be reobtained for nonzero  $\Gamma_0$  by redefining constants and rescaling variables. There is a general arbitrariness in the choices of constants for both light and dark beams. Our choices are such as to facilitate comparisons with the numerical results of Ref. [11]. Soliton solutions correspond to strict equality on the right-hand side of Eq. (7), yielding

$$b_z^2 = 2 \left[ b^2 - b_m^2 - (1 + b_m^2) \ln \frac{1 + b^2}{1 + b_m^2} \right]. \tag{8}$$

This equation describes an antisymmetric beam with finite intensity at infinity and a narrow dark region in the middle.

The more general solutions, such that the constant  $b_{z0}^2$  is less than its soliton value, once again correspond to periodic structures. We will consider them in what follows. When the constant  $b_{z0}^2$  is only slightly smaller than its soliton value in either Eq. (5) or (6), the solutions look like corresponding solitons locally, but are periodic on a larger scale (soliton trains).

### III. STABILITY

To study the stability of any of the solutions of Sec. II, we consider superimposing periodic modulations in  $y$  on them such that

$$B(x, y, z) = [b(z) + \delta b(x, z) \sin(ky)] e^{i\Gamma_0 x}. \tag{9}$$

Here  $\delta b$  is assumed to be small. We obtain a system of equations linear in  $\delta b$ ,

$$\begin{aligned} & \left( -i \frac{\partial}{\partial x} - \frac{1}{2} \frac{\partial^2}{\partial z^2} - s \frac{b^2 - b_0^2}{1 + b^2} + \Gamma_0 \right) \delta b \\ & = -\frac{1}{2} k^2 \delta b + s b \phi + \text{c.c.}, \end{aligned} \tag{10}$$

$$\begin{aligned} & \frac{\partial^2}{\partial z^2} \phi - k^2 \phi + \frac{\partial}{\partial z} \left[ \phi \frac{\partial}{\partial z} \ln(1 + b^2) \right. \\ & \left. - \frac{1 + b_0^2}{1 + b^2} \frac{\partial}{\partial z} \left( \frac{b(\delta b + \delta b^*)}{1 + b^2} \right) \right] = 0, \end{aligned} \tag{11}$$

where  $\phi = \partial \delta \phi / \partial z$ . We look for solutions such that  $\delta b = \delta b^{(1)} e^{\gamma x} + \delta b^{(2)} e^{\gamma^* x}$ . As the above equations involve both  $\delta b$  and  $\delta b^*$ , just taking  $e^{\gamma x}$  terms, as some authors do, would be too restrictive. (Results so obtained would only be valid for  $\gamma^2 > 0$ .) When  $\gamma > 0$ , perturbations will grow along  $x$  and the ground-state solution is unstable. It will break up. Here we will find  $\gamma(k)$  for small  $k$ , in which parameter we will expand all perturbed quantities and  $\gamma$ :

$$\gamma = \gamma_1 k + \gamma_2 k^2 + \dots, \tag{12a}$$

$$\delta b = \delta b_0 + k \delta b_1 + \dots, \tag{12b}$$

$$\phi = \phi_0 + k \phi_1 + \dots. \tag{12c}$$

Equations simplify for  $\eta = \delta b^{(1)} + \delta b^{(2)*}$  and  $\chi = \delta b^{(1)} - \delta b^{(2)*}$ . At each stage of the calculation we eliminate  $\phi_n$ . It can be seen by inspection that there will be two dis-

tinct perturbed modes: (i)  $\chi_0, \eta_1, \chi_2, \eta_3, \dots$  and all  $\chi_{2n+1}, \eta_{2n}$  zero and (ii)  $\eta_0, \chi_1, \eta_2, \chi_3, \dots$  with  $\chi_{2n}, \eta_{2n+1}$  zero. These modes couple for more general  $\mathbf{k}$  (not along  $y$ ); see [3,4]. From now on, we will consider the two classes of light beam,  $s = +1$  and  $s = -1$ , separately.

### A. Bright beams

For bright beams,  $s = 1$ ,  $b_0 = 0$ , and  $b_z^2$  is given by Eq. (5). We now take  $b_{z0}^2 = 0$  and expand Eqs. (10) and (11), expressed in terms of  $\eta, \chi, \phi$ , in  $k$ . In zeroth order we have

$$L \eta_0 = 0, \quad L' \chi_0 = 0, \quad (13)$$

$$L = L' + \frac{2b^2}{(1+b^2)^2}, \quad L' = \frac{1}{2} \frac{\partial^2}{\partial z^2} + \frac{b^2}{1+b^2} - \Gamma_0. \quad (14)$$

These equations are solved by  $\eta_0 = \alpha b_z$  and  $\chi_0 = \beta b$ , where  $\alpha, \beta = \text{const}$ . As mentioned above, the two modes  $\alpha = 0, \beta \neq 0$  and  $\alpha \neq 0, \beta = 0$  decouple. It transpires that the type-2 mode ( $\beta = 0$ ) is stable,  $\gamma^2 < 0$ . For type 1, due to linearization, we can take  $\beta = 1$ . For solitons, for which perturbed quantities vanish at infinity, we have in first order

$$L \eta_1 = -i \gamma_1 \chi_0, \quad (15)$$

$$\eta_1 = -i \gamma_1 b_z \int \frac{z b^2}{b_z^2} dz, \quad (16)$$

$$\phi_1 = \frac{b \eta_1}{(1+b^2)^2}. \quad (17)$$

Here the integral in  $\eta_1$  is a principal value.

In second order we obtain

$$L' \chi_2 = -i \gamma_1 \eta_1 + \frac{1}{2} b. \quad (18)$$

Multiplying Eq. (18) by  $\chi_0 = b$ , the eigenfunction of  $L'$ , on the left and integrating over all  $z$ , using the self-adjoint property of  $L'$ , and reinstating  $k$ , we obtain

$$\frac{\gamma^2}{k^2} = - \frac{\langle b^2 \rangle}{\langle b^4 / b_z^2 \rangle} > 0. \quad (19)$$

The integral in the denominator is a principal value integral and will be seen to be negative.

Objections have been raised about the rigor of soliton stability calculations such as the above. These objections concern the behavior of higher-order perturbed quantities at infinity [17]. Various remedies have been suggested [3,18–20]. One of these remedies [18] involves performing the stability analysis for periodic nonlinear waves, for which the calculation is rigorous, and then finding the soliton limit of  $\gamma$ . In our case  $b_{z0}^2 < 0$  should be taken in Eq. (5) and  $b_{z0}^2 \rightarrow 0$  in the limit. This has been done by us. Equation (19) is reobtained. The calculation is fairly complicated and will not be included here. Chapter 8 of Ref. [4] illustrates how to do the calculation (though in a different context).

Instead of calculating  $\gamma/k$  from Eqs. (5) and (19), we will use a model for the soliton shape. This model will be a hyperbolic secans squared fit to Eq. (5) with  $b_{z0}^2 = 0$ . The

amplitude will of course be  $b_m$ . The other parameter will be chosen such that the shape near the maximum is preserved. Thus  $b_z^2 / (b_m^2 - b^2)$  will be taken to be a perfect fit for small  $b_m^2 - b^2$ . Next we must check to see how good a fit the model so constructed is over the whole range of  $b$  for given  $b_m^2$ .

The model so defined is

$$b = b_m \cosh^{-2}(\sigma z), \quad (20a)$$

$$\sigma^2 = \frac{1}{b_m^2} \ln(1 + b_m^2) - \frac{1}{1 + b_m^2}, \quad (20b)$$

$$b_z^2 = 4\sigma^2 (b^2 - b_m^{-1} b^3). \quad (20c)$$

Figure 1 gives a comparison of exact and model soliton shapes in phase space  $b_z^2(b^2)$ . Agreement on the right is exact. Otherwise it is seen to be very good for  $b_m^2 = 1$ , reasonable for  $b_m^2 = 2$ , but its usefulness seems to end just before or at  $b_m^2 = 4$ . Figure 1 thus tells us just how good our model (20) is and just how well we are justified in using it. In a subsequent paper, we plan to perform the stability calculation for the exact profile and compare results. However, Fig. 1 leads us to expect reasonable results of our stability analysis for  $0.5 \leq b_m^2 \leq 4$ . With all this in mind, we substitute Eq. (20) into Eq. (19) to obtain an approximate equation for  $\gamma/k$  in the bright soliton case

$$\frac{\gamma}{k} = \frac{2}{\sqrt{3}} \sqrt{b_m^{-2} \ln(1 + b_m^2) - (1 + b_m^2)^{-1}}, \quad (21a)$$

$$0.5 \leq b_m^2 \leq 4 \quad (21b)$$

(in arriving at this result we use the principal value equality  $\text{Pf} \int_{-\infty}^{\infty} \sinh^{-2} z dz = -2$ ). The formula obtained from the exact profile would not be so simple. If an experimentalist needs a quick check, Eq. (21a) may prove useful.

Figure 2 illustrates this dependence on  $b_m^2$ . There is a saturation as compared with the nonlinear Schrödinger equation (Kerr medium), for which  $\gamma/k \sim b_m$  [3]. In Ref. [11(b)], a numerical calculation was performed and  $\gamma(k)$  deduced for  $k > 0.05$  (small  $k$  cannot be treated numerically, as simulations must be performed in boxes, the lengths of which are limited by practical considerations). In Ref. [11],  $b_m^2$  was taken to be 0.5, 1, 2, and 4, thus coinciding with the region of applicability of our model. In Fig. 1 of Ref. [11],  $\gamma(k)$  is not extended into the small- $k$  region. However, it is possible to find the range of values of  $\gamma/k$  that would continue their dispersion curves smoothly into this small- $k$  region. This range is indicated in our Fig. 2 as a rectangle. We see that our result (21) is consistent with and complementary to existing numerical results.

Only approximate agreement with numerical results can be expected for a second reason, other than the use of a model for the soliton shape. As mentioned above, numerical calculations are always performed in finite boxes, usually with periodic boundary conditions. Thus the results of Ref. [11] are really found for a soliton train rather than for one soliton, stretching out to plus and minus infinity. We will return to this point in the next section, where it will play an important role.

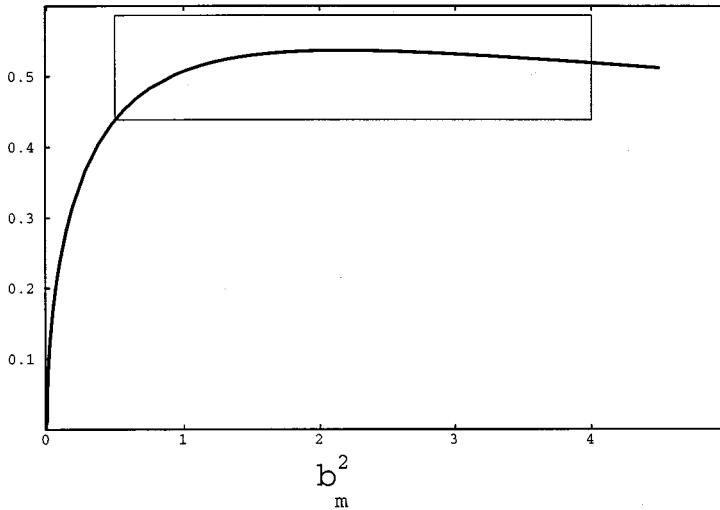
$\gamma/k$ 

FIG. 2. Growth rate  $\gamma/k$  for small  $k$  as a function of  $b_m^2$  for the bright soliton. The rectangle embraces values that could follow from the numerical simulations of Ref. [11] when continued smoothly into the small- $k$  region.

### B. Dark beams

For dark beams, Eq. (8), type-1 perpendicular perturbations are stable. However, type-2 perturbations are unstable for nonlinear periodic and soliton structures: Eq. (6),  $b_{z0}^2$  smaller than or equal to the soliton value. We now treat these structures.

Now Eqs. (10) and (11) yield ( $s = -1$ ,  $b_0 = b_m$ ,  $\Gamma_0 = 0$ )

$$L = L' - \frac{2(1+b_m^2)}{(1+b^2)^2} b^2, \quad (22)$$

$$L' = \frac{1}{2} \frac{\partial^2}{\partial z^2} + \frac{b_m^2 - b^2}{1+b^2}, \quad (23)$$

$$L\eta_0 = 0, \quad \eta_0 = b_z, \quad \chi_0 = 0. \quad (24)$$

In first order in  $k$  we have

$$L'\chi_1 = -i\gamma_1 b_z, \quad \chi_1 = -i\gamma_1 b \int \frac{z b^2 - \langle b^{-2} \rangle^{-1}}{b^2} dz \quad (25)$$

(the second term in the integral has been added so as to remove the secularity). The angular brackets now denote an average over a period of the nonlinear structure.

In second order we find

$$\phi_2 = \frac{1+b_m^2}{(1+b^2)^2} b \eta_2 + \frac{\sigma}{2(1+b^2)} \int^z (b^2 - \langle b^2 \rangle) dz, \quad (26a)$$

$$L\eta_2 = -i\gamma_1 \chi_1 + \frac{1}{2} \eta_0 + \frac{\sigma b}{1+b^2} \int^z (b^2 - \langle b^2 \rangle) dz, \quad (26b)$$

where

$$\sigma = \frac{1+b_m^2}{1+\langle b^2 \rangle}.$$

When we substitute Eq. (25) in Eq. (26b) and multiply by  $\eta_0$  on the left and then perform the integrations by parts, we obtain, reinstating  $k$ ,

$$\frac{\gamma^2}{k^2} = \frac{-\langle b_z^2 \rangle + \sigma \langle \ln(1+b^2)(b^2 - \langle b^2 \rangle) \rangle}{\langle b^2 \rangle - \langle b^{-2} \rangle^{-1}}. \quad (27)$$

As before,  $\langle b^{-2} \rangle$  is a principal value integral. By manipulating Eqs. (4) and (6), we can find its value in terms of non-singular integrals

$$\langle b^{-2} \rangle = b_{z0}^{-2} \left[ \langle b_z^2 \rangle + 2\langle b^2 \rangle + 2(1+b_m^2) \left( \left\langle \frac{\ln(1+b^2)}{b^2} \right\rangle - 1 \right) \right]. \quad (28)$$

In the soliton limit we obtain ( $\sigma = 1$ )

$$\frac{\gamma^2}{k^2} = \frac{-\langle b_z^2 \rangle + \left\langle \ln \left( \frac{1+b^2}{1+b_m^2} \right) (b^2 - b_m^2) \right\rangle}{\left\langle \frac{(b^2 - b_m^2)^2}{b^2} \right\rangle} > 0. \quad (29)$$

Now integration is over the whole  $z$  axis. It is easy to see that  $\gamma^2/k^2 > 0$  for the soliton, as the integrand of the numerator is everywhere negative, and the denominator (a principal value) is also negative. To see that Eq. (29) follows from Eq. (27), we write the latter in an equivalent form

$$\frac{\gamma^2}{k^2} = \frac{-\langle b_z^2 \rangle + \sigma \left\langle \ln \left( \frac{1+b^2}{1+b_m^2} \right) (b^2 - \langle b^2 \rangle) \right\rangle}{\left\langle (b^2 - b_m^2) \left( \frac{b^2 - \langle b^{-2} \rangle^{-1}}{b^2} \right) \right\rangle}. \quad (30)$$

We calculated  $\gamma^2/k^2$  for five values of  $b_m^2$ . Figure 3 shows this ratio as a function of  $\lambda$ , the wavelength of the nonlinear structure. This wavelength is given by

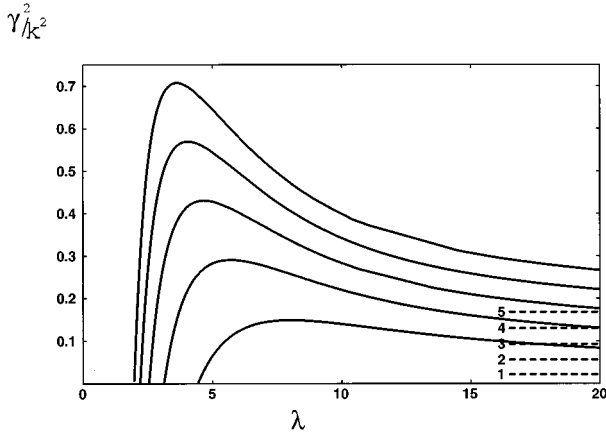


FIG. 3. Squared growth rate  $\gamma^2/k^2$  for dark stripes in periodic nonlinear structures (dark soliton trains). Here the ordinate denotes the wavelength  $\lambda$ . Soliton values for  $\lambda \rightarrow \infty$  are indicated by dashed lines.

$$\lambda = 2\sqrt{2} \int_0^a \frac{db}{\sqrt{b^2 - (1 + b_m^2)\ln(1 + b^2) + \frac{1}{2}b_{z0}^2}}, \quad (31)$$

where  $a$  is the first zero of the square root. Values of  $\lambda$  extend from  $\sqrt{2}\pi/b_m$  in the linear limit to infinity in the soliton limit. The amplitude  $a$  increases monotonically with  $\lambda$  for  $b_m$  fixed.

As  $\gamma^2/k^2 > 0$ , one root is positive and we have instability for all  $\lambda$ . We see from Fig. 3 that growth rates for solitons are much smaller than for nonlinear wave structures in the displayed range of  $\lambda$ . Two dispersion curves, based on Eq. (27), were seen to tend to limits given by Eq. (29) when continued beyond the range of Fig. 3. This is an additional check on the calculations.

In Ref. [11(a)], numerical calculations for nonlinear structures that the authors label *solitons* are performed. Instability is obtained and growth rates are calculated for  $b_m^2 = 2$  and 4. Their growth rates, when extrapolated into the small- $k$  region, would be at least three times larger than ours, as shown in Fig. 3. As numerical simulations are always performed in

finite boxes, normally with periodic boundary conditions, we propose to explain the disparity by assuming that the simulations of Ref. [11] really correspond to nonlinear, periodic solutions (soliton trains). Furthermore, Fig. 3 strongly suggests that the value for  $b_m^2 = 4$  should be larger than for  $b_m^2 = 2$ , contrary to Ref. [11]. We contacted one of the authors of Ref. [11] and suggested that perhaps they had confused the two labels. This was indeed confirmed after consultation with a second author [21].

#### IV. CONCLUSION

It is hoped that our two main results, Eqs. (21) and (27), will prove useful when designing optical beams to propagate along photorefractive media. Stability properties can be improved by moving to the right on a constant  $b_m$  curve (this would involve narrowing the dark center and broadening the light envelope) or else decreasing  $b_m$  for constant  $\lambda$  (decreasing the brightness of the envelope while keeping its length fixed). Presumably it would be worthwhile to confirm these propositions experimentally.

Experimental observations of Ref. [11] do point at perpendicular instability of the beams. Other scientists, however, find the beams to be stable with respect to  $y$  perturbations. This has been observed for both dark [22] and bright [23] solitons. Just why the instability appears in some experiments and not in others is so far an open question.

We can, however, confirm at least one experimental finding. We can see from Fig. 3 that structures that do not fit into the soliton profile (wrong ratio of width to height, curves to the left of soliton limits) are much more unstable with respect to symmetry breaking than the solitons. This is indeed what was found in Refs. [22,23].

#### ACKNOWLEDGMENTS

The authors would like to thank Dr. Saffman and Dr. Zozulya for helping clear up the apparent discrepancy described in Sec. III. Dr. Skorupski was most helpful in preparing the manuscript. Professor Rowlands' comments were most useful. This research was supported by the KBN Scientific Committee, Grant No. 2P03B-114-11.

- 
- [1] V. E. Zakharov and A. B. Shabat, Zh. Eksp. Teor. Fiz. **61**, 118 (1971) [Sov. Phys. JETP **34**, 62 (1972)].
- [2] V. E. Zakharov and A. M. Rubenchik, Zh. Eksp. Teor. Fiz. **65**, 997 (1973) [Sov. Phys. JETP **38**, 494 (1974)].
- [3] E. Infeld and G. Rowlands, Z. Phys. B **37**, 277 (1980).
- [4] E. Infeld and G. Rowlands, *Nonlinear Waves, Solitons and Chaos* (Cambridge University Press, Cambridge, United Kingdom, 1992).
- [5] P. Frycz and E. Infeld, Phys. Rev. Lett. **63**, 384 (1989).
- [6] P. Frycz, E. Infeld, and J. C. Samson, Phys. Rev. Lett. **69**, 1057 (1992).
- [7] E. Infeld, A. Senatorski, and A. A. Skorupski, Phys. Rev. Lett. **72**, 1345 (1994).
- [8] E. Infeld, A. Senatorski, and A. A. Skorupski, Phys. Rev. E **51**, 3183 (1995).
- [9] A. Senatorski and E. Infeld, Phys. Rev. Lett. **77**, 2855 (1996).
- [10] A. V. Mamaev *et al.*, Phys. Rev. A **54**, 870 (1996).
- [11] (a) A. V. Mamaev, M. Saffman, and A. A. Zozulya, Phys. Rev. Lett. **76**, 2262 (1996); (b) Europhys. Lett. **35**, 25 (1996).
- [12] F. Vidal and T. V. Johnston, Phys. Rev. Lett. **77**, 1282 (1996).
- [13] M. Segev *et al.*, Phys. Rev. Lett. **73**, 3211 (1994).
- [14] A. A. Zozulya and P. Z. Anderson, Phys. Rev. A **51**, 1520 (1995); D. N. Christodoulides and M. I. Carvallio, J. Opt. Soc. Am. B **12**, 1628 (1995).
- [15] M. Segev, M. F. Shih, and G. C. Valley, J. Opt. Soc. Am. B **13**, 706 (1996).

- [16] V. Tihonenko, J. Christou, and B. Luther-Daves, *J. Opt. Soc. Am. B* **12**, 2046 (1995).
- [17] E. Infeld and G. Rowlands, *Plasma Phys.* **19**, 343 (1977).
- [18] E. Infeld, *J. Plasma Phys.* **33**, 171 (1985).
- [19] M. A. Allen and G. Rowlands, *J. Plasma Phys.* **50**, 413 (1993).
- [20] M. A. Allen and G. Rowlands, *J. Plasma Phys.* **53**, 63 (1995).
- [21] M. Saffman (private communication).
- [22] Z. Chen *et al.*, *Opt. Lett.* **21**, 629 (1996).
- [23] K. Kos *et al.*, *Phys. Rev. E* **53**, R4330 (1996); Z. Chen *et al.*, *Opt. Lett.* **21**, 1436 (1996).